Estimating the Fraction of Winter Orographic Precipitation Produced under Conditions Meeting the Seeding Criteria for the Wyoming Weather Modification Pilot Project

JACLYN M. RITZMAN* AND TERRY DESHLER

University of Wyoming, Laramie, Wyoming

KYOKO IKEDA AND ROY RASMUSSEN

National Center for Atmospheric Research,+ Boulder, Colorado

(Manuscript received 3 July 2014, in final form 13 February 2015)

ABSTRACT

Annual precipitation increases of 10% or more are often quoted for the impact of winter orographic cloud seeding; however, establishing the basis for such values is problematic for two reasons. First, the impact of glaciogenic seeding of candidate orographic storms has not been firmly established. Second, not all winter precipitation is produced by candidate ''seedable'' storms. Addressing the first question motivated the Wyoming state legislature to fund a multiyear, crossover, randomized cloud-seeding experiment in southeastern Wyoming to quantify the impact of glaciogenic seeding of wintertime orographic clouds. The crossover design requires two barriers, one randomly selected for seeding, for comparisons of seeded and nonseeded precipitation under relatively homogeneous atmospheric conditions. Addressing the second question motivated the work here. The seeding criteria—700-hPa temperatures $\leq -8°C$, 700-hPa winds between 210° and 315°, and the presence of supercooled liquid water—were applied to eight winters to determine the percent of winter precipitation that may fall under the seeding criteria. Since no observational datasets provide precipitation and all of the atmospheric variables required for this study, a regional climate model dynamical downscaling of historical data over 8 years was used. The accuracy of the model was tested against several measurements, and the small model biases were removed. On average, ~26% of the time between 15 November and 15 April atmospheric conditions were seedable over the barriers in southeastern Wyoming. These seedable conditions were accompanied by precipitation ~12%–14% of the time, indicating that ~27%–30% of the winter precipitation resulted from seedable clouds.

1. Introduction

Augmenting the winter snowpack through glaciogenic seeding has been considered since artificial ice nuclei were shown to produce ice crystals in clouds containing supercooled liquid water (SLW; Schaefer 1946; Vonnegut 1947). Orographic clouds, which develop when air is cooled by being forced up and over a mountain barrier, are often targeted for wintertime glaciogenic cloud seeding since they contain SLW and frequently occur throughout the winter months over complex terrain (Politovich and Vali 1983; Boe and Super 1986; Hindman 1986; Rauber et al. 1986). Glaciogenic seeding's ability to augment the winter snowpack has been tested through randomized seeding experiments (RSEs; Grant and Mielke 1967; Mielke et al. 1971; Morel-Seytoux and Saheli 1973; Elliott et al. 1978; Super and Heimbach 1983), and through physical experiments to measure changes in cloud microphysics due to seeding (Deshler et al. 1990; Deshler and Reynolds 1990; Geerts et al. 2010, 2013; Pokharel et al. 2014a,b; Pokharel and Geerts 2014). Many of these physical experiments sought after and focused on the best possible seedable conditions.

While physical experiments are useful to document possible physical changes within seeded clouds, they are

* Current affiliation: NOAA/NWS/Weather Forecast Office, Wichita, Kansas.

+ The National Center for Atmospheric Research is sponsored by the National Science Foundation.

Corresponding author address: Jaclyn Ritzman, 2142 S. Tyler Road, Wichita, KS 67209.
E-mail: jaclyn.ritzman@noaa.gov

DOI: 10.1175/JAMC-D-14-0163.1

not useful to provide an overall estimate of annual precipitation change because the frequency of such conditions over the winter is unknown, the number of cases is limited, and, in most papers, the cases presented are selected by the authors to provide the most interesting and most positive seeding effects. Thus, RSEs are required to quantify the impact over a winter; however, RSEs suffer from a lack of statistically significant results because of the limited number of years in an experiment and/or unanticipated errors in experimental design or execution. Results from RSEs are expressed in statistical form through a percent change, between seeded and nonseeded precipitation, and a probable certainty (Gabriel 1999). For precipitation impact feasibility studies, the percent change between seeded and nonseeded precipitation in previous studies is then typically applied to the total wintertime precipitation to estimate the overall effect of glaciogenic seeding (e.g., Griffith et al. 2007). This approach makes the assumption that all wintertime precipitation arises from storms that meet seedable conditions, which is unlikely. To more accurately assess the benefits of glaciogenic seeding, the percent change due to glaciogenic seeding should only be applied to seedable precipitation events.

One of the first RSEs in the western United States was the Climax experiment in northern Colorado. The promising results of Climax I (Grant and Mielke 1967), an exploratory experiment, led to Climax II (Mielke et al. 1971), a confirmatory experiment. Climax I showed a positive seeding effect, especially through the first half of the experimental cases. Further analysis by Mielke et al. (1970) showed a 6%–11% increase in seeded precipitation; however, obtaining these results by chance alone could not be ruled out. The initial Climax II analysis (Mielke et al. 1971; Chappell et al. 1971) showed results similar to the Climax I experiment; however, high seeded to nonseeded precipitation ratios upwind of the treated areas led Mielke (1979) to statistically reanalyze Climax I and II data. The conclusions were that the results were statistically insignificant and that positive seeding results could have been due to a lucky draw of the cases treated. Mielke et al. (1981) then changed the day of the control station measurements for Climax I and II and found statistically significant evidence of a positive seeding effect, albeit a smaller magnitude. The Mielke et al. (1981) reanalysis was rebutted by Rhea (1983) who found that the results from Mielke et al. (1981) were not statistically significant when the control and target data were synchronized more accurately.

Although Climax brought about controversial results (Rhea 1983; Rangno and Hobbs 1987, 1993) and sparked several additional reanalyses, this inaugural RSE was important and many lessons were learned and applied in current seeding operations. Following the promising results at the time, the Climax I experiment sparked additional RSEs, the Lake Almanor experiment (Mooney and Lunn 1969), the confirmatory Climax II experiment (Mielke et al. 1971; Chappell et al. 1971), the Wolf Creek Pass Experiment (Morel-Seytoux and Saheli 1973), the Colorado River Basin Pilot Project (Elliott et al. 1978), and the Bridger Range Experiment (Super and Heimbach 1983). Most of the above-mentioned RSEs utilized long, problematic treatment periods, as seeding took place for up to 24 h in most experiments. These long treatment periods were problematic as atmospheric conditions can vary significantly over such extended periods of time and include conditions unfavorable for seeding in the analyses of project results (Rangno 1986). These early RSEs also investigated potential seedable conditions, for example, 700-hPa temperatures, 500-hPa temperatures, cloud-top temperatures, and various wind directions. Cloud-top temperatures were initially thought to be a crucial atmospheric variable for glaciogenic seeding of orographic clouds (Grant and Elliott 1974); however, Rangno (1979) and Hobbs and Rangno (1979) showed that cloud-top temperatures have a poor correlation with in-cloud temperatures, which are the temperatures important for activation of the artificial ice nuclei used. Although the aforementioned RSEs have shown a positive seeding effect, results are still questioned and controversial. A National Research Council review of studies of the augmentation of wintertime snowfall due to glaciogenic seeding concluded that scientifically sound evidence of snowpack augmentation was not available (Garstang et al. 2003). This conclusion was also not without controversy (Garstang et al. 2005). With variations in previous results, a lack of scientifically conclusive results, and/or potential flaws in experimental designs, the impact of glaciogenic seeding on the wintertime snowpack remains to be successfully proven.

In 2008 the Wyoming Weather Modification Pilot Project (WWMPP), a multiyear RSE, began in southeastern Wyoming to extend and improve upon earlier glaciogenic RSEs and investigate the benefits of glaciogenic seeding to aide in the alleviation of drought conditions. The experimental design improved upon earlier RSEs by refining the seeding criteria and significantly shortening the treatment periods to 4 h. The goal of the multiyear effort, and short time period for experimental cases, was to obtain enough comparisons of seeded and nonseeded precipitation to reach statistical significance.

While the goal of the WWMPP is to test for a change between seeded and nonseeded precipitation, it leaves unaddressed the percent of time and precipitation amount that occurs under seedable conditions. To extend project results more broadly, this paper addresses

the question of what percent of the wintertime snowpack over the WWMPP RSE study area would be considered seedable. This question is addressed by applying the WWMPP RSE seeding criteria to 8 years of simulated meteorological conditions over the study area. Limitations of reanalysis data required the use of simulated meteorology to obtain all atmospheric variables used in the WWMPP. The simulated data are from an 8-yr regional dynamical downscaling of historical data produced by the Weather Research and Forecasting (WRF) Model over the headwaters of the Colorado (Ikeda et al. 2010; Rasmussen et al. 2014).

Hill (1974) discussed the percent of seedable precipitation in Utah and provided an estimate of ~30%. Elliott et al. (1978) state that 35% of the seasonal snowpack between 15 October and 15 May fell on experimental days, and hence conditions were seedable according to specified criteria. Medina (2000) estimated that ~45% of the snowpack in the Park Range in Colorado is seedable, based on simulations of seven storms in the winter of 1998/99 using the Colorado State University Regional Atmospheric Modeling System. To our knowledge these are the only published studies addressing the subject of this paper, the percent of wintertime precipitation amenable to treatment with artificial ice nuclei.

2. The Wyoming Weather Modification Pilot Project

To limit the time required to reach statistical significance, the WWMPP RSE was designed as a randomized crossover experiment, requiring two very similar barriers. The two barriers chosen were the Sierra Madre (SM) range and the Medicine Bow mountain range (MB) in southeastern Wyoming separated by the Saratoga Valley. At the same time as the WWMPP RSE, ground-based generator seeding began over the Wind River Range in central Wyoming, 200 km northwest of the SM, in an exploratory physical experiment. This was not a part of the RSE. The crossover design stipulates that for a 4-h seeding case to begin, seedable atmospheric conditions must be present and forecast to persist for a minimum of 4 consecutive hours over both barriers simultaneously. Once conditions were forecast to become seedable and SLW was present, a radiosonde was launched from Saratoga, Wyoming, to verify the 700-hPa wind direction and temperature. If atmospheric conditions were suitable, the 4-h seeding case was started. This resulted in paired (one barrier seeded and the other not seeded) 4-h cases in which seeded and nonseeded precipitation occurred under relatively homogeneous atmospheric conditions. The precipitation target areas were located on both mountain ranges near Snow Telemetry (SNOTEL) sites, provided by the U.S. Department of Agriculture Natural Resource Conservation Service. These SNOTEL sites were at Old Battle in the SM and Brooklyn Lake in the MB. Multiple high-resolution precipitation gauges were located near these SNOTEL sites to provide precipitation measurements used within the WWMPP RSE evaluation process.

The artificial ice nuclei used in the WWMPP RSE are silver iodide (AgI) particles. The AgI particles are introduced into the atmosphere via ground-based generators upwind of the barriers, allowing ambient flow to transport the artificial ice nuclei into the target orographic clouds, while the other barrier remains nonseeded. The seeded barrier is selected randomly. Except for necessary operational personnel, the seeding decisions are kept confidential. Therefore, individuals involved in analyzing project results have no knowledge of the seeding decisions, limiting potential bias.

The experimental design, seeding criteria, and the planned statistical evaluation for the WWMPP RSE are described in detail by Breed et al. (2014). The experiment targets orographic clouds when 700-hPa temperatures are $\leq -8°C$, 700-hPa winds are westerly between 210° and 315°, and SLW is present and expected to persist. The presence of SLW is a key criterion for seeding, as glaciated clouds without SLW have no potential for seeding. The 700-hPa temperature limit was established from measurements of AgI activation as a function of temperature (DeMott 1997). The 700-hPa wind directions were established through examination of previous precipitation events due to orographic lift using SNOTEL data and 700-hPa wind directions from National Weather Service atmospheric sounding data at Riverton, Wyoming (Weather Modification Incorporated 2005). A sharp uptick (downtick) in precipitation events over the SM occurred under westerly (easterly) flow at 700 hPa. This relationship of wind and precipitation is reinforced and confirmed later on in this study.

The temperature constraints limit the WWMPP RSE operations to the period of 15 November–15 April. Weather Modification Incorporated handles seeding operations and the National Center for Atmospheric Research is responsible for the statistical evaluation, deployment, and maintenance of precipitation gauges and other instrumentation required for seeding decisions, as well as supporting the forecasting and case-calling team by running a high-resolution version of WRF, utilizing real-time four-dimensional data assimilation. In addition to these main components, snow chemistry sampling is performed by the Desert Research Institute and streamflow modeling by the University of Alabama. In parallel to the RSE, and under external funding, microphysical

measurements using aircraft were made by the University of Wyoming. The experimental and data collection phase of the WWMPP RSE was completed in April 2014. Results of the RSE will be formally made available in autumn of 2015, when the final report is provided to the Wyoming Water Development Commission and Legislative Select Water Committee of the Wyoming State Legislature (see the acknowledgements section of the present paper for disclaimer information regarding these WWMPP data and the results and conclusions of the present paper).

3. Datasets

Analyzing the percent of seedable precipitation requires a long-term temporally resolved (4 h or less) dataset of precipitation with corresponding atmospheric measurements of temperature, wind direction, and SLW. The North American Regional Reanalysis (NARR) data (Mesinger et al. 2006) contain temperature and wind direction, but lack an SLW variable and adequate spatial resolution over both barriers. Possible NARR variables to establish an SLW surrogate were explored and compared with radiometer measurements of SLW, but none were found to be suitable (Ritzman 2013). Hoover et al. (2014) discuss deficiencies of the NARR over complex, mountainous terrain. Although SNOTEL data are available over both barriers, the temporal resolution is not consistent prior to 2006, and is generally too coarse. From 2000 to 2006 Brooklyn Lake SNOTEL data are reported between 2 and 6 times a day, and at Old Battle SNOTEL between 6 and 8 times a day, depending on the water year. Resolving precipitation events over both barriers simultaneously would be extremely difficult at best. With the NARR dataset lacking an appropriate SLW variable or surrogate, and SNOTEL data lacking temporal consistency, a regional model dataset, created by dynamical downscaling of historical data for the headwaters of the Colorado, was investigated (Ikeda et al. 2010; Rasmussen et al. 2011, 2014). Early work presented by Rhea (1978) demonstrated hydrometeorological applications of modeling over complex terrain. Data from well-performed simulations can be a good surrogate for observational measurements.

The model dataset contains all necessary atmospheric variables and precipitation data at high temporal (hourly) and spatial (4 km) resolutions. This dataset was created to test the ability of WRF to reproduce the wintertime snowpack over complex terrain (Ikeda et al. 2010; Rasmussen et al. 2011, 2014). The simulation was run for 2000–08. The model domain is shown in Fig. 1. The WRF Model was forced and updated every 3 h utilizing the 32-km NARR data. The Thompson et al. (2008) microphysics scheme was utilized and provided mixing ratios for vapor, cloud water, rainwater, graupel, ice, and snow. Further details of the WRF configuration can be found in Rasmussen et al. (2014).

To check the model dataset for accuracy and bias, the data are compared to measurements. SNOTEL data allow weekly accumulations of precipitation and overall seasonal accumulations to be compared against WRF precipitation over the WWMPP RSE target areas for every year of the model simulation. There is one year of overlap between the model dataset and the WWMPP field measurements, the winter of 2007/08 when instruments were deployed prior to the beginning of the RSE to finalize project details. The WWMPP field measurements of interest here consist of SLW radiometer measurements over the MB and 75 atmospheric soundings released from Saratoga, Wyoming. Therefore, SNOTEL precipitation, radiometer, and atmospheric sounding measurements will form the basis of the comparisons with the model.

a. *Precipitation*

Ikeda et al. (2010) tested the ability of WRF to reproduce the wintertime snowpack over the Colorado Headwaters region and found that with a horizontal grid spacing of less than 6 km, WRF performed well and produced snowfall agreeable to SNOTEL measurements. For comparisons to the two SNOTEL sites in the WWMPP RSE target areas, simulated WRF precipitation at model grid points surrounding the SNOTEL site was used to compute inverse-distance weighted average values. Over the SM three of the four closest grid points were used. The grid point excluded was on the downsloping side of the SM, where, as would be expected, consistently lower precipitation estimates were found compared to the other three grid points. Terrain over the MB is broader near the summit, allowing for all four of the closest grid points to be used.

Underestimation of snowfall measurements, utilizing weighing gauges surrounded by an Alter shield, can range from 10% to 15% depending on wind speeds in forest clearings where gauges are typically sited (Yang et al. 1998; Serreze et al. 1999; Rasmussen et al. 2001, 2012). The SNOTEL measurements, which use weighing gauges, are reported with an accuracy of 2.5 mm and the sites in the SM and MB are in wind prone forest clearings. Thus, underestimations will affect the comparisons. To show the potential biases in SNOTEL data, both 10% and 15% underestimations, due to unaccounted wind bias, are used to provide a more realistic comparison against WRF precipitation. Unfortunately, SNOTEL precipitation gauges do not have collocated anemometers.

For a quantitative analysis, weekly cumulative and 8-yr climatological averaged precipitations were calculated

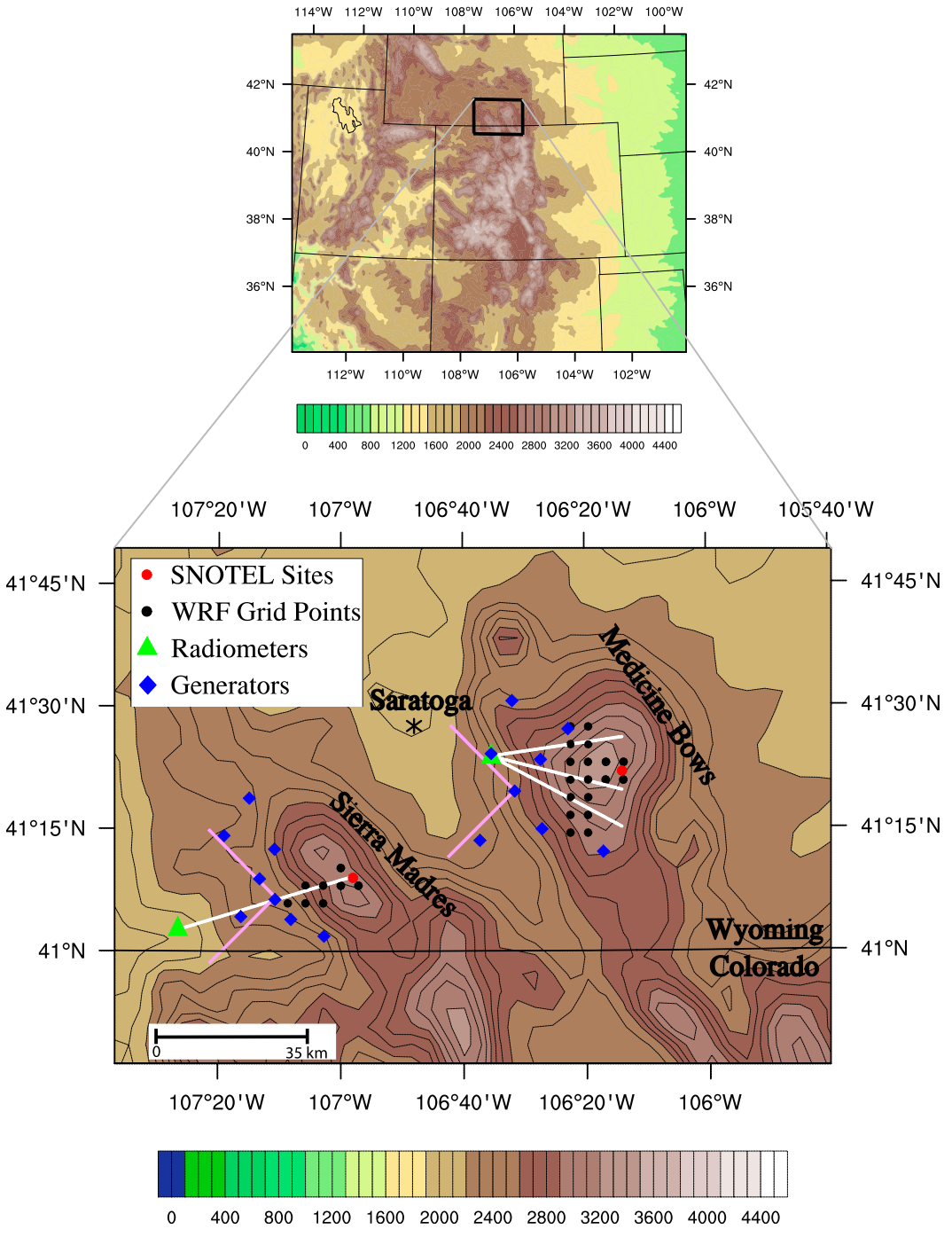

FIG. 1. Plan view of the 4-km WRF domain with terrain height color filled and contoured in 100-m intervals. The maximum contour levels over the SM and MB are 3000 and 3200 m, respectively. (top) The region containing the SMs and MBs is outlined in black. (bottom) The zoomed-in plan view shows the WWMPP RSE seeding generators, radiometer locations, WRF grid points, SNOTEL sites, and radiometer azimuth paths in white lines. In pink lines, the wind directions in which the WWMPP operates are highlighted. At the bottom-left corner, a scale bar has been included.

from the WRF and SNOTEL data. For SNOTEL data, the 8-yr climatological average precipitation was computed based on the daily precipitation data first, then weekly total precipitation was determined for the individual 24 weeks between 1 November and mid-April for each season. For the WRF data, the hourly model output was used to determine the 8-yr climatological average. Then, the weekly precipitation amounts were

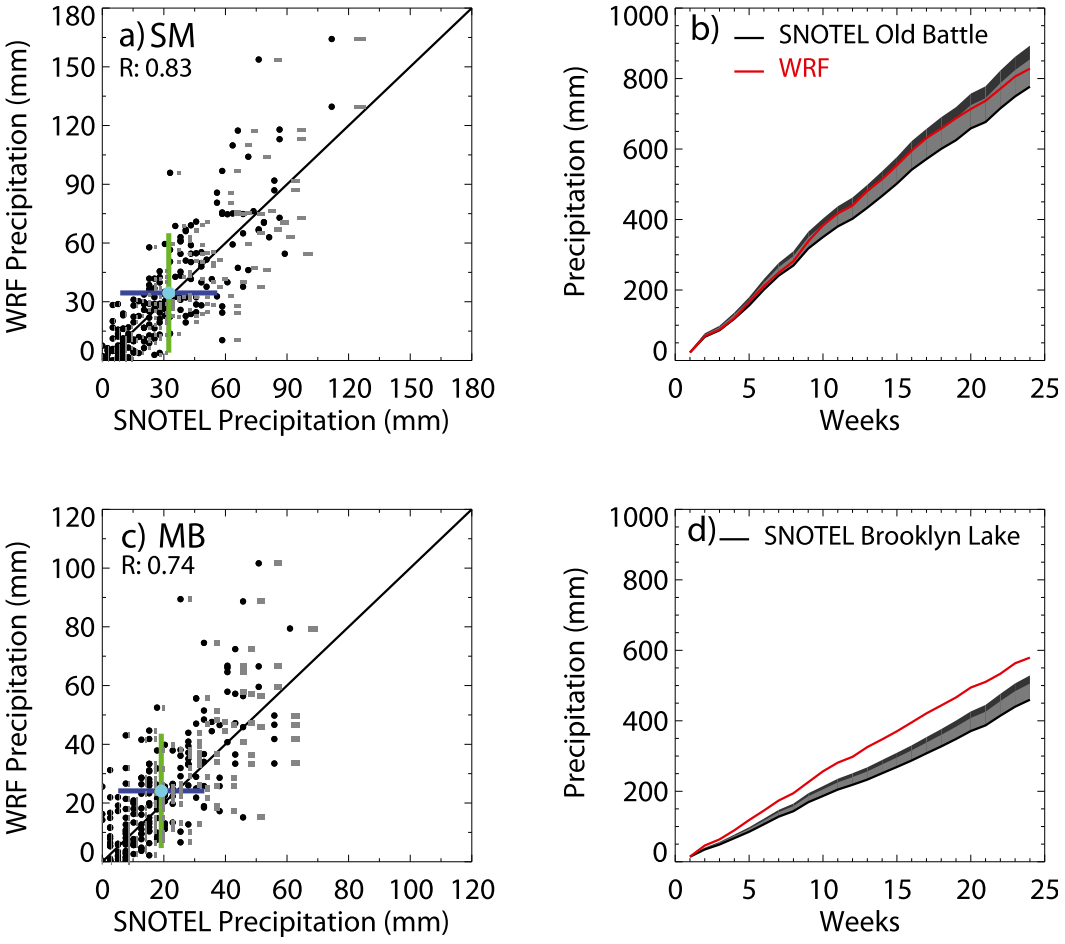

FIG. 2. Scatterplots of WRF and SNOTEL weekly accumulations over the (a) SM and (c) MB between 1 Nov and mid-April 2000–08. The correlation coefficients, averages in cyan dots, std dev for WRF (SNOTEL) in green vertical (blue horizontal) lines, and a 1:1 solid black line are plotted. The SNOTEL underestimation for each of these weekly accumulations is represented by the gray rectangles spanning 10%–15% errors. The 8-yr average seasonal precipitation accumulations are given for the (b) SM and (d) MB. SNOTEL measurements are in solid black, and WRF estimates are in red. The 10% (15%) underestimation of SNOTEL measurements are shown in light (dark) gray shading.

found for the 24 individual weeks. Dividing the annual precipitation into weekly amounts limits a bias from any one storm significantly affecting the overall comparison, and provides 192 individual comparisons.

The 192 comparisons for the SM (MB) are shown in Fig. 2a (Fig. 2c). SNOTEL and WRF weekly accumulations of precipitation are well correlated over the SM (MB) with a correlation coefficient of 0.83 (0.74). When SNOTEL data are corrected for the potential 10%–15% underestimation, it is noticeable that these corrections move the WRF precipitation data closer to the 1:1 line in most instances. Over the MB precipitation events are less intense than over the SM in both simulated and observed data. Perhaps in the dominant westerly flow regime the moisture encounters the SM first and thus less moisture is available to the MB, located downwind from the SM.

Averaging weekly precipitation for the 8 comparison years and accumulating the precipitation over the 24 weeks leads to the overall comparison of seasonal precipitation shown in Fig. 2b (Fig. 2d) for the SM (MB). This seasonal cumulative precipitation analysis is closer to the traditional method of examining SNOTEL measurements than the weekly precipitation analysis. On average, WRF performed well at reproducing the temporal trend of precipitation events. The WRF Model reproduced precipitation near the SM target area quite well, lying between the actual SNOTEL measurements and SNOTEL data corrected for the 15% undercatch and nearly overlaps the 10% underestimation error. WRF

precipitation near the MB target area diverges quickly from the SNOTEL measurements, and both the 10% and 15% underestimation errors are insufficient after a few weeks to bring the data back into agreement. Nevertheless, the temporal trends in precipitation events are still captured. With overall good agreement with observations, the simulated WRF precipitation data, inverse-distance weighted to the WWMPP target locations in the SM and MB, were used to determine hourly precipitation events for the analysis in sections 4 and 5.

b. SLW

The MB radiometer measures the amount of liquid water (LW) present along a slant path and converts this to a vertical integral of the LW per unit area. The LW is termed SLW if the temperature is below 0°C. MB radiometer azimuths (Fig. 1) are scanned continuously to intersect orographic clouds that develop because of particular wind directions: 80° for northwest flow, 110° west flow, and 135° southwest flow. To allow comparison with radiometer measurements, LW was calculated using WRF data by integrating the cloud and rainwater mixing ratios [see Eq. (1) below]. The units of Eq. (1) were then converted from meters to millimeters to match the units of the radiometer data for comparison. Converting this integral in altitude to an integral over pressure, using the hydrostatic equation, leads to

$$\mathrm{LW} = \frac{1}{g\rho_w} \int r_w(p)\, dp, \qquad (1)$$

where r_w is the cloud LW mass mixing ratio ($\mathrm{kg\,kg^{-1}}$), which results from the addition of the cloud and rainwater mixing ratios; g is the acceleration of gravity; and ρ_w is the density of water. Pressure levels p that intersect the beam of the MB radiometer slant paths at the up- and downwind grid points determine the pressure limits for the integration. The calculation of LW was initially examined at individual grid points, along the three specific azimuths, and over an area of grid points encompassing all three azimuths.

To obtain maximum coverage of the three different MB radiometer azimuths, WRF LW was calculated utilizing the area of grid points shown in Fig. 1. This calculated WRF LW is compared in a time series and difference analysis to MB radiometer data in Fig. 3. In general, the WRF simulation does quite well in capturing LW events, both in time and magnitude. On average, radiometer measurements, which fell within ±10 min of the WRF-simulated LW, were 0.012 mm lower than the LW simulated by the WRF, but with a standard deviation 6 times this amount. In most cases, there is a lag in the WRF-simulated LW as the cyan dots tend to be negative and then positive through LW events. Away from these periods, during times devoid of LW the datasets present good agreement.

The WWMPP RSE does not specify a threshold of SLW for seeding to take place, but only that SLW is present and forecast to remain so. According to Fig. 3, WRF does a good job of identifying the cases when SLW was present in March 2008. Since these results provide confidence in the ability of the WRF Model to simulate LW over the MB, with a reasonable temporal fidelity, using the WRF LW to satisfy the SLW seeding criterion over the MB seems reasonable.

There are no SM radiometer data coincident with the WRF simulations, so no verification over the SM was performed. Considering that the WWMPP RSE requires SLW over both barriers, and that reasonable agreement was found over the MB, WRF LW was calculated for the SM over an area of grid points that encompass the single azimuth in which the SM radiometer operates. Figure 1 shows the grid points that were used in the WRF LW calculation [Eq. (1)], described in this section, for both barriers to determine whether the SLW criterion was met for the analysis in sections 4 and 5.

c. 700-hPa temperature and wind direction

The 75 atmospheric soundings from Saratoga (Fig. 1) were taken between 29 November 2007 and 26 February 2008. To compare temperatures and wind directions, the differences were determined as WRF data minus sounding measurements. The atmospheric soundings were matched to the closest hour of WRF data. The differences from the 75 comparisons are shown in Fig. 4a (Fig. 4b) for the 700-hPa temperatures (wind directions). The averages of the differences at 700 hPa indicate WRF has a cold bias of 0.9°C and overestimates the wind direction by 11°. To determine whether the 700-hPa temperature and wind direction seeding criteria were met for the analysis in sections 4 and 5, the WRF temperatures and wind directions were averaged over each barrier, using the WRF grid points shown in Fig. 1, and the biases that have been discussed were removed.

4. Seeding criteria application

Before applying the seeding criteria to the hourly WRF data, the calculated WRF LW and bias-corrected 700-hPa temperatures and wind directions were used to construct histograms of the seeding criteria for the entire dataset and for data only during precipitation events over the WWMPP RSE target areas in Fig. 5. The only requirement for a precipitation event over the WWMPP RSE target areas was an hourly accumulation of greater than zero. Considering the entire WRF dataset between

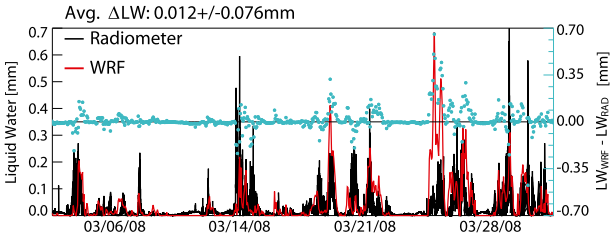

FIG. 3. The left *y* axis corresponds to the time series analysis of simulated WRF and measured LW. The LW over the MB in black is measured by the radiometer at Cedar Creek for March 2008. Data from the three azimuth angles are shown as one black line as the radiometer rotates through all three azimuths sequentially, and the radiometer baseline has been removed. WRF simulation of cloud LW over the MB for the radiometer scan angles is shown in red. WRF grid points used to calculate WRF LW are specified in Fig. 1 and encompass all three radiometer azimuths. The right *y* axis corresponds to the cyan dots and shows the difference between WRF-simulated and radiometer-measured LW applying a ±10-min threshold. The average difference and std dev are indicated above the figure.

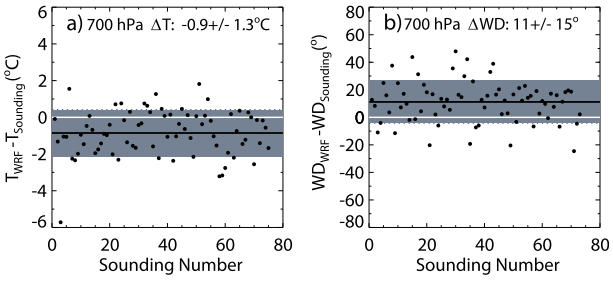

FIG. 4. Comparisons between 75 Saratoga soundings and WRF-simulated data for 700-hPa (a) temperature and (b) wind direction. Solid white lines represent zero, solid black lines represent the average difference, and the gray shaded area indicates one std dev. The average difference and std dev are also indicated at the top.

15 November and 15 April, approximately 55% of the time SLW occurs over and immediately upwind of both the SM and MB (Figs. 5a,d), 40% of the time 700-hPa temperatures are ≤−8°C (Figs. 5b,e), and 60%–70% of the time the wind direction is between 210° and 315° (Figs. 5c,f). Overall, the 700-hPa temperatures are the most limiting factor for seeding, and wind directions are the least limiting factor. During precipitation events, there are instances when clouds did not contain LW throughout an hour of precipitation over both barriers. However, ~90% of the time precipitation occurred under conditions when LW was present for the entire hour (Figs. 5a,d). Approximately 50% of the time precipitation occurred temperatures were ≤−8°C (Figs. 5b,e), while the distributions of wind for all WRF data and for WRF data with precipitation are almost identical. Examining each criterion individually clearly shows that the 700-hPa temperature is the most limiting criterion. The similarity of the results for both barriers indicates that the SM and MB are excellent targets for glaciogenic seeding through the WWMPP RSE seeding criterion and the two barriers were good candidates for a crossover RSE. Also, Figs. 5c and 5f show that the majority of wintertime precipitation events fall under westerly 700-hPa winds, which was discussed earlier in determining the appropriate wind directions for the WWMPP RSE.

Though the histograms in Fig. 5 show how each individual WWMPP RSE seeding criterion is distributed across the WRF data, to determine a seedable percent of precipitation and time, the criteria must be met simultaneously. The WWMPP RSE seeding criteria were applied simultaneously to every hour of WRF-simulated data, by requiring that all three criteria are met at the beginning and end of each hour. Thus, each potential seeding period is 1 h in duration. This was done to ensure that for the entire hour, the temperature was cold enough for AgI to nucleate, wind direction was favorable for the lofting and transport of AgI, and SLW was present. This will result in total time amenable for seeding for each of the 8 years of simulation data. Comparison with the total time from 15 November to 15 April will provide a seedable percentage of time. This percentage can be further subdivided into those hours with and without precipitation.

5. Seedable precipitation results

Figure 6a shows the percent of time without (with) precipitation in brown (blue) when the WWMPP RSE seeding criteria were met between 15 November and 15 April, within the 8-yr WRF simulation for the SM and MB. The percent of time in which seedable atmospheric conditions were present for the 8 years ranged from a high of ~39% in 2007/08 to a low of 18% in 2006/07, while the averages over both barriers were nearly the same at ~26% of the time. Limiting the results to only time periods when there was precipitation over the target areas reduces the time by about 50% to ~12%–14%. Thus approximately half of the time when seedable atmospheric conditions are present, precipitation does not fall over the target areas. For the 8-yr simulation, on average 952 (947) hours of seedable atmospheric conditions were present over the SM (MB) from 15 November to 15 April, while the average number of hours of seedable atmospheric conditions accompanied by precipitation over the SM (MB) was 498 (455).

More important, the seedable percent should be determined as a function of total precipitation during the winter seeding season. The season with the most seedable precipitation for the SM (MB) was 2003/04 (2001/02) with ~35% (~42%). The season with the least

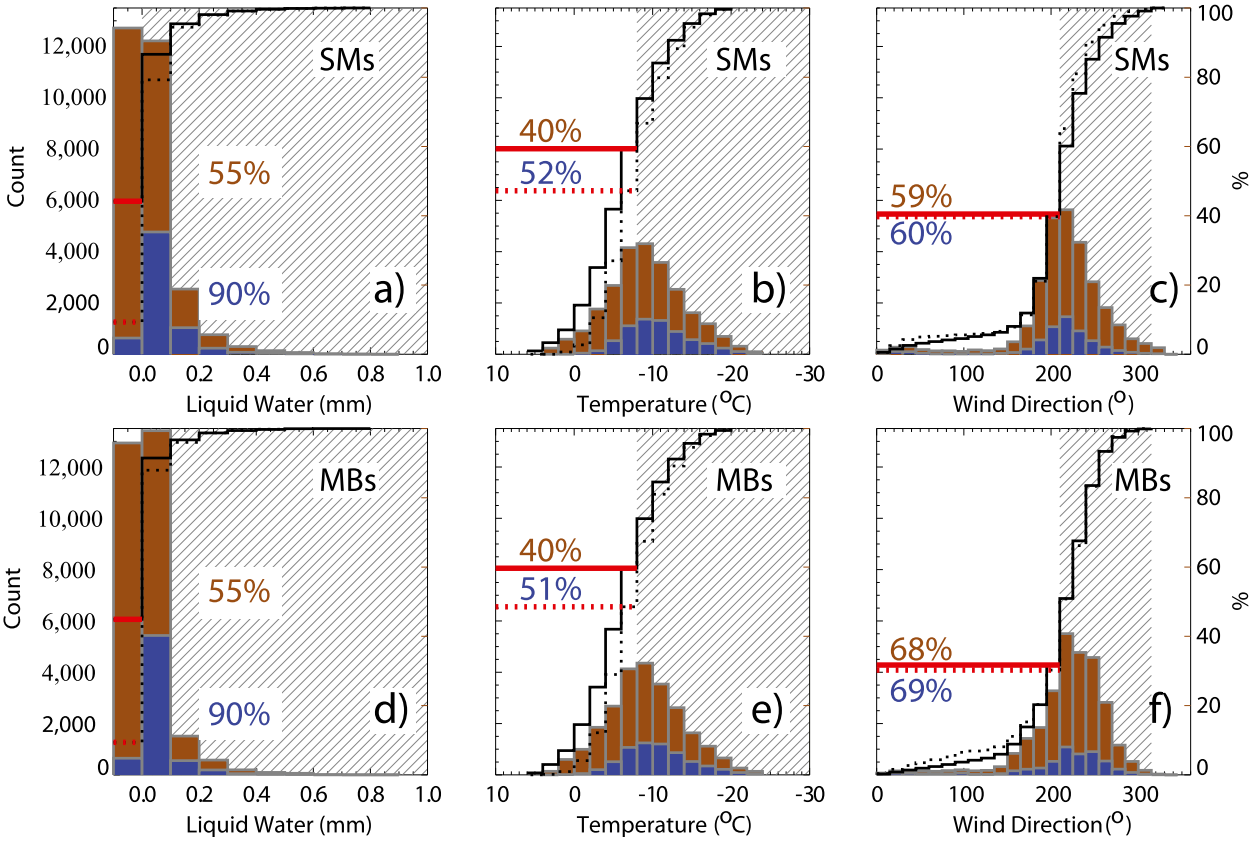

FIG. 5. Histograms for LW amounts, 700-hPa temperature, and 700-hPa wind direction over the (a)–(c) SM and (d)–(f) MB between 15 Nov and 15 Apr 2000–08 using hourly WRF data. Histograms in brown are for all WRF data, while those in blue are for WRF data during all precipitation events. Bins to the left of 0.0 in (a) and (d) represent precipitation events when LW was not present throughout the entire hour. The hatched areas denote the WWMPP RSE seeding criteria. The cumulative percent of events distributed by the three seeding criteria is shown in black lines—solid for all data and dotted for data during precipitation events. The percent of time when the WRF data did not meet individual seeding criteria is given at the point the cumulative percent meets the hatched area. These points are shown by red horizontal lines—solid for all WRF data and dotted for WRF data during precipitation events. The seedable fraction in each category is given by 100 minus these values and is provided in brown for all WRF data and blue for WRF data during precipitation events.

seedable precipitation for both barriers occurred in 2004/05 with ~12%–13% of the snowpack being qualified as seedable.

On average, over the SM, seedable atmospheric conditions were present ~26% of the time and ~14% of the time when precipitation was occurring. This ~14% equates to ~27% of the wintertime snowpack from 15 November to 15 April being seedable. Over the MB, the numbers are quite similar. Seedable atmospheric conditions were present ~26% of the time, and of this time precipitation was occurring ~12% of the time. This ~12% equates to ~30% of the wintertime snowpack from 15 November to 15 April being seedable.

To provide a level of uncertainty with the model-simulated LW, the same aforementioned analysis was performed over the SM and MB, but omitting the LW requirement and only applying the 700-hPa temperature and wind direction criteria (Fig. 6b). This analysis increased the average percent of time seedable atmospheric conditions occurred by ~12%–14%, to ~38%–40%. However, the average percent of time seedable atmospheric conditions were present and precipitation fell over the target area only increased slightly by ~2%–3%, to ~15%–16%. These small increases also increased the average percent of seedable precipitation by ~4%–5%, to ~31%–35%.

To provide a bit of historical context against previous seeding experiments, cloud-top temperatures were analyzed for all clouds and for seedable clouds (Fig. 7). A top-down analysis along the model vertical direction was performed to obtain the temperature when the following cloud properties first appeared and were greater than zero in the WRF data: cloud liquid water, rainwater, ice, snow, and/or graupel mixing ratios. The model data, initially on model sigma levels in the vertical, were interpolated at 50-hPa increments and extends

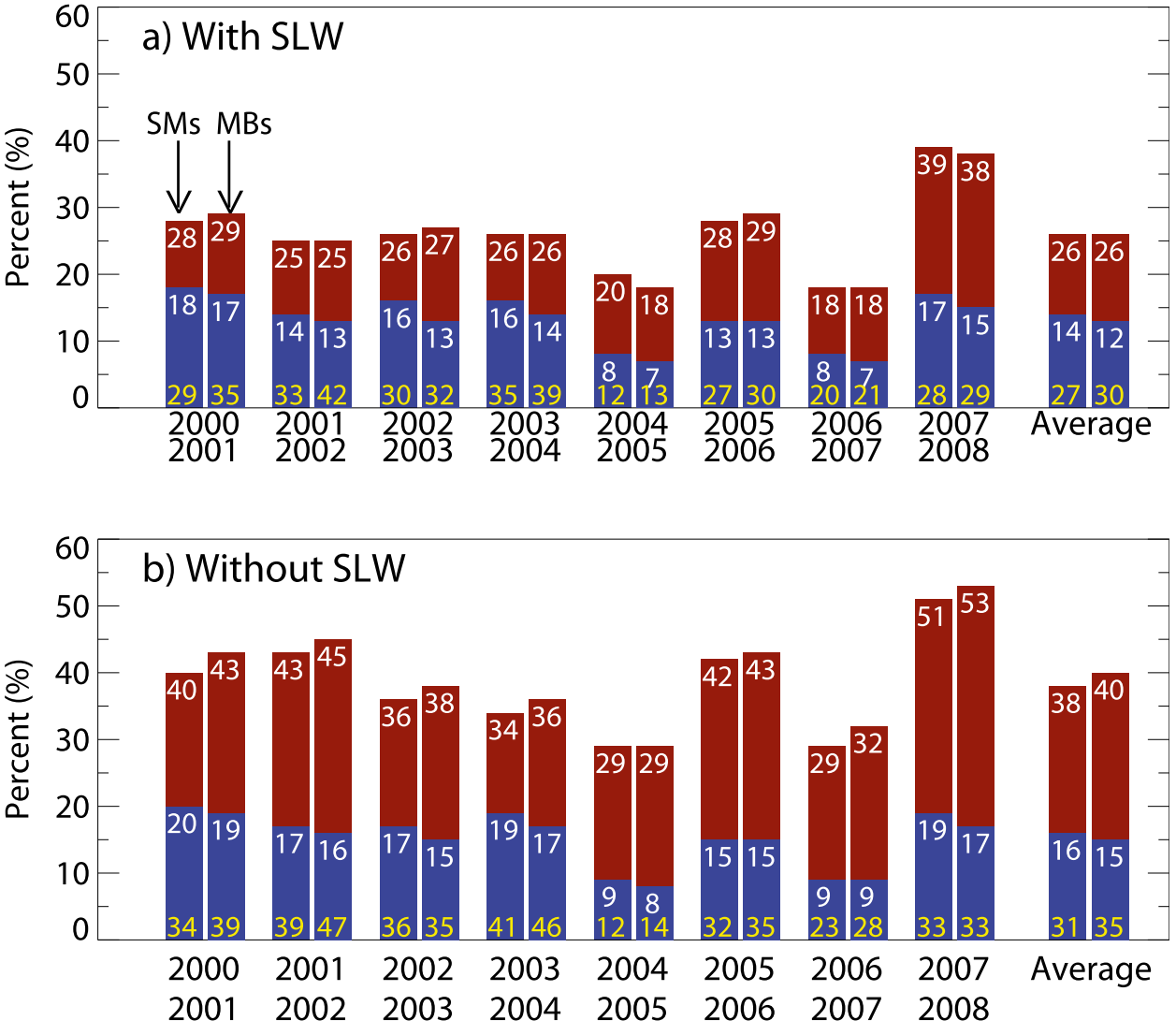

FIG. 6. The percent of time between 15 Nov and 15 Apr (a) when simulated conditions met all three requirements for seeding, SLW, 700-hPa temperature, and wind direction, in the SM and MB and (b) when the requirement for SLW was removed. Each year and the 8-yr average for the MB and SM are shown. The first (second) column for each season is for the SM (MB). The brown shaded areas and value at the top are for all data under seedable conditions, while blue is restricted to seedable conditions when precipitation was also being simulated over the WWMPP RSE target areas. The yellow percentages located at the bottom of the blue bars represent the percent of the simulated snowpack that accumulated under seedable conditions.

up to 300 hPa. Early research suggested that seedable cloud-top temperatures ranged from −10° to −25°C (Grant and Elliott 1974). Approximately half of the seedable clouds determined through this analysis fell within the category from −10° to −25°C. This distribution of cloud-top temperatures suggests that approximately half of the seedable clouds might have had plenty of natural ice or might have been influenced by clouds above because the top-down approach will always assign cloud-top temperatures from the first or highest cloud encountered, although neither of these possibilities can be confirmed.

Another question not yet addressed in this analysis, but required by streamflow modelers, is the overall effect of glaciogenic seeding over the whole barrier. Figure 8 partially addresses this issue by providing the spatial distribution of the frequency of SLW from model grid points over and upwind of the WWMPP RSE target areas for seedable conditions with and without precipitation. For example, the farthest southwest grid point upwind of the MB had simulated SLW over that particular grid point 90% (78%) of the time when precipitation fell (did not fall) over the RSE target area under seedable conditions. During seedable atmospheric

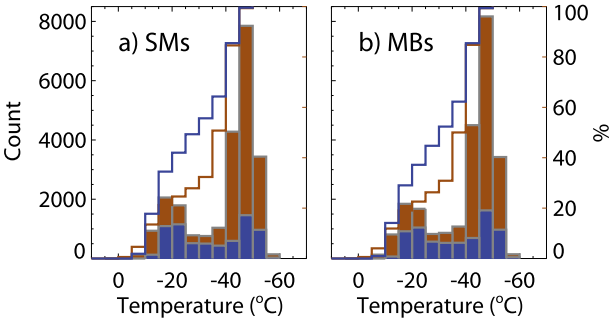

FIG. 7. Histograms, in 5°C increments, of cloud-top temperature during all cloud events in brown and seedable cloud events in blue over the (a) SM and (b) MB. Cumulative distributions of the cloud-top temperature for these cases are shown in brown solid lines for all clouds and in blue solid lines for seedable cloud events, with scale on the right.

conditions when precipitation fell over the WWMPP RSE target areas, the highest (lowest) percentage of time when SLW was present occurred along the western (eastern) flank of the MB. Over the SM the distribution is slightly more uniform. The rain-shadow effect is very apparent, with the percentages dropping off rapidly immediately downwind of the MB crest. During non-precipitation seedable atmospheric conditions, the western flanks maintain the largest areal coverage of the SLW.

With approximately 27%–30% of the snowpack being impacted by glaciogenic cloud seeding, statistical results of snowpack augmentation potential from RSEs cannot be applied to an entire snowpack. Applying the result arrived at here to the 10% increase in precipitation often stated in previous weather modification studies reduces these estimates to an increase of ~2.7%–3% of the total precipitation. The results here, along with results from the WWMPP RSE (Breed et al. 2014), will be used to arrive at an overall effect of weather modification on the wintertime snowpack through streamflow modeling incorporating seedable dates and times from this analysis. The number of cases for which seedable conditions did not persist for more than 1 total hour was very minimal and did not have a large impact on overall results.

The percent of seedable precipitation determined through the work presented here is close to the amount stated by Hill (1974) and Elliott et al. (1978); however, the results are less than Medina (2000). This is expected as Medina (2000) only used the LW criterion, which is the least limiting factor, for seven storms during 1998/99. However, the seasons with the highest amount of seedable precipitation in the MB and SM approach the seedable amount of precipitation presented in Medina (2000).

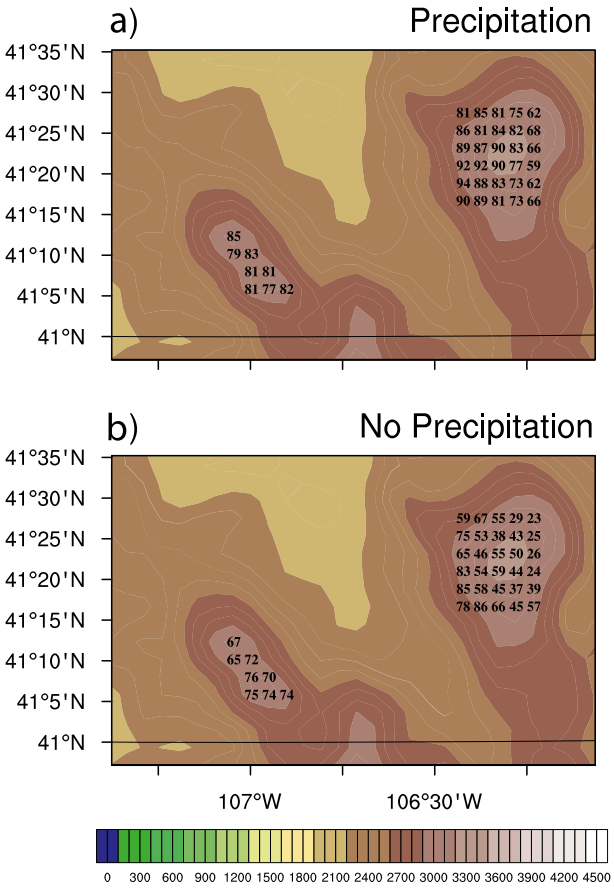

FIG. 8. The frequency of SLW for each grid point over the SM and MB is shown during seedable atmospheric conditions when precipitation (a) occurred or (b) did not occur over the RSE target areas. The seedable conditions were determined based on the seeding criteria—700-hPa temperatures, 700-hPa wind directions, and SLW—from grid points shown in Fig. 1; however, more grid points are shown here to show the larger spatial variability.

Not only do these results show that the amount of seedable precipitation can vary by more than a factor of 2 from winter to winter, but they also indicate that not all seedable atmospheric conditions are coupled with precipitation. Approximately half of the time atmospheric conditions were seedable according to WWMPP RSE seeding criteria; however, no precipitation occurred over the target areas. These atmospheric conditions add to the seeding potential over the SM and MB. It is important that operational glaciogenic seeding projects do not wait for snowfall to occur over target areas prior to seeding as this may limit the potential to affect clouds that are not producing natural precipitation.

6. Summary and conclusions

The percentage of precipitation that may result from conditions appropriate for seeding wintertime orographic

clouds was assessed over the Sierra Madre and the Medicine Bow mountain range in southeastern Wyoming. This was done as part the Wyoming Weather Modification Pilot Project randomized seeding experiment. The definition of a seedable cloud was based on the seeding criteria for the experiment: 700-hPa temperatures $\leq -8°C$, 700-hPa winds between 210° and 315°, and the persistent presence of SLW. No reanalysis data were available that contain all of these variables at the necessary temporal and spatial resolution to carry out the sufficient investigations. Thus the analysis depended on an 8-yr dynamical downscaling simulation, forced by reanalysis data, over the Colorado Headwaters using the Weather Research and Forecasting Model at a 4-km spatial resolution from 2000 to 2008 (Ikeda et al. 2010; Rasmussen et al. 2014). As a first step to this study, the simulated data were compared with available measurements from precipitation gauges, atmospheric soundings, and a radiometer.

In comparison with SNOTEL data, WRF-simulated precipitation data reproduced the wintertime snowpack and its temporal trends quite well over the target areas. The WRF 700-hPa temperatures and winds were compared with 75 atmospheric soundings from Saratoga, Wyoming, over the 2007/08 winter season. The comparisons revealed that WRF had a slight cold bias of $<1°C$ and that WRF winds had a slight northerly bias. Both of these model biases were taken into account before applying the seeding criteria to the model data. The modeled supercooled liquid water was found to capture the temporal evolution and rough magnitude of liquid water observed by a radiometer looking over the Medicine Bow.

Analyzing the 8 years of simulated data over both barriers in southeastern Wyoming from 15 November to 15 April, utilizing the randomized experiment's seeding criteria, led to estimates of the 1) percent of time when seedable clouds were present, 2) percent of time when seedable clouds were present and precipitation occurred over target areas, and 3) percent of seedable precipitation over target areas. From 2000 to 2008 the average percent of the wintertime snowpack that would have been seedable was ~27%–30%, while for any one winter the seedable percent ranged from ~12% to 42%. The average amount of time when seedable atmospheric conditions were present over the barriers was ~26%. About half of the time when atmospheric conditions were considered seedable no precipitation fell over the WWMPP RSE target areas. Since there have been questions about the accuracy of the model estimates of SLW, and SLW was determined to be the least restrictive criteria, the analysis was also performed using only the 700-hPa temperature and wind direction criteria. This additional analysis increased the amount of seedable precipitation to ~31%–35% and the amount of time when seedable atmospheric conditions were present over the barriers to ~38%–40%. On the basis of the seedable percentages of precipitation over both target areas, it is clear that applying a percent change in precipitation due to seeding to an entire winter snowpack would significantly overestimate the benefit that could accrue as a result of seeding, because not all wintertime precipitation is seedable.

Dates and times of seedable precipitation events have been provided to streamflow modelers to assist in bridging the gap between the statistical results of the Wyoming Weather Modification Pilot Project and the targeted streamflow augmentation that may accrue. This allows for a more accurate evaluation of the benefits and costs of operational glaciogenic seeding utilizing the seeding criteria applied for this experiment.

Acknowledgments. The authors thank and acknowledge the state of Wyoming and the Wyoming Water Development Commission for the funding to perform this research, Weather Modification Incorporated, for providing atmospheric sounding data from Saratoga, the National Center for Atmospheric Research for providing the WRF and radiometer data, and the U.S. Department of Agriculture Natural Resource Conservation Service for the SNOTEL data. All rights to the underlying data collected and/or generated with funding from the Wyoming Water Development Office (WWDO) from which this report was created, remain with the WWDO. This report does not constitute the opinions of the State of Wyoming, the Wyoming Water Development Commission or the Wyoming Water Development Office.

REFERENCES

Boe, B. A., and A. B. Super, 1986: Wintertime characteristics of supercooled liquid water over the Grand Mesa of western Colorado. *J. Wea. Modif.,* **18,** 102–107.

Breed, D., R. Rasmussen, C. Weeks, B. Boe, and T. Deshler, 2014: Evaluating winter orographic cloud seeding: Design of the Wyoming Weather Modification Pilot Project (WWMPP). *J. Appl. Meteor. Climatol.,* **53,** 282–299, doi:10.1175/JAMC-D-13-0128.1.

Chappell, C. F., L. O. Grant, and P. W. Mielke Jr., 1971: Cloud seeding effects on precipitation intensity and duration of wintertime orographic clouds. *J. Appl. Meteor.,* **10,** 1006–1010, doi:10.1175/1520-0450(1971)010<1006:CSEOPI>2.0.CO;2.

DeMott, P. J., 1997: Report to North Dakota Atmospheric Resource Board and Weather Modification Incorporated on tests of the ice nucleating ability of aerosols produced by the Lohse

airborne generator. Colorado State University Department of Atmospheric Science Rep., 15 pp.

Deshler, T., and D. W. Reynolds, 1990: The persistence of seeding effects in a winter orographic cloud seeded with silver iodide burned in acetone. *J. Appl. Meteor.,* **29,** 477–488, doi:10.1175/1520-0450(1990)029<0477:TPOSEI>2.0.CO;2.

——, ——, and A. W. Huggins, 1990: Physical response of winter orographic clouds over the Sierra Nevada to airborne seeding using dry ice or silver iodide. *J. Appl. Meteor.,* **29,** 288–330, doi:10.1175/1520-0450(1990)029<0288:PROWOC>2.0.CO;2.

Elliott, R. D., R. W. Shaffer, A. Court, and J. F. Hannaford, 1978: Randomized cloud seeding in the San Juan Mountains, Colorado. *J. Appl. Meteor.,* **17,** 1298–1318, doi:10.1175/1520-0450(1978)017<1298:RCSITS>2.0.CO;2.

Gabriel, K. R., 1999: Ratio statistics for randomized experiments in precipitation simulations. *J. Appl. Meteor.,* **38,** 290–301, doi:10.1175/1520-0450(1999)038<0290:RSFREI>2.0.CO;2.

Garstang, M., and Coauthors, 2003: *Critical Issues in Weather Modification Research.* National Academies Press, 123 pp.

——, R. Bruintjes, R. Serafin, H. Orville, B. Boe, W. Cotton, and J. Warburton, 2005: Weather modification: Finding common ground. *Bull. Amer. Meteor. Soc.,* **86,** 647–655, doi:10.1175/BAMS-86-5-647.

Geerts, B., Q. Miao, Y. Yang, R. Rasmussen, and D. Breed, 2010: An airborne profiling radar study of the impact of glaciogenic cloud seeding on snowfall from winter orographic clouds. *J. Atmos. Sci.,* **67,** 3286–3302, doi:10.1175/2010JAS3496.1.

——, and Coauthors, 2013: The AgI Seeding Cloud Impact Investigation (ASCII) campaign 2012: Overview and preliminary results. *J. Wea. Modif.,* **45,** 24–43.

Grant, L. O., and P. W. Mielke, 1967: A randomized cloud seeding experiment at Climax, CO, 1960–1965. *Proceedings of the Fifth Berkeley Symposium on Mathematical Statistics and Probability,* L. M. Le Cam and J. Neyman Eds., Vol. 5, University of California Press, 115–131.

——, and R. E. Elliott, 1974: The cloud seeding temperature window. *J. Appl. Meteor.,* **13,** 355–363, doi:10.1175/1520-0450(1974)013<0355:TCSTW>2.0.CO;2.

Griffith, D. A., M. E. Solak, D. P. Yorty, and B. Brinkman, 2007: A level II weather modification feasibility study for winter snowpack augmentation in the Salt and Wyoming Ranges in Wyoming. *J. Wea. Modif.,* **39,** 76–83.

Hill, G. E., 1974: Precipitation augmentation potential by cloud seeding in the state of Utah. Rep. 428, 45 pp. [Available online at http://digitalcommons.usu.edu/cgi/viewcontent.cgi?article=1427&context=water_rep.]

Hindman, E. E., 1986: Characteristics of supercooled liquid water in clouds at mountaintop sites in the Colorado Rockies. *J. Climate Appl. Meteor.,* **25,** 1271–1279, doi:10.1175/1520-0450(1986)025<1271:COSLWI>2.0.CO;2.

Hobbs, P. V., and A. L. Rangno, 1979: Comments on the Climax and Wolf Creek Pass cloud seeding experiments. *J. Appl. Meteor.,* **18,** 1233–1237, doi:10.1175/1520-0450(1979)018<1233:COTCAW>2.0.CO;2.

Hoover, J. D., N. Doesken, K. Elder, M. Laituri, and G. E. Liston, 2014: Temporal trend analyses of alpine data using North American Regional Reanalysis and in situ data: Temperature, wind speed, precipitation, and derived blowing snow. *J. Appl. Meteor. Climatol.,* **53,** 676–693, doi:10.1175/JAMC-D-13-092.1.

Ikeda, K., and Coauthors, 2010: Simulation of seasonal snowfall over Colorado. *Atmos. Res.,* **97,** 462–477, doi:10.1016/j.atmosres.2010.04.010.

Medina, J. G., 2000: The feasibility of operational cloud seeding in the North Platte River basin headwaters to increase mountain snowfall. Bureau of Reclamation Denver Federal Center Technical Service Center Rep., 115 pp. [Available online at https://platteriverprogram.org/PubsAndData/ProgramLibrary/TC-R5%20Feasibility%20of%20Cloud%20Seeding%20in%20North%20Platte%20Headwaters.pdf.]

Mesinger, F., and Coauthors, 2006: North American Regional Reanalysis. *Bull. Amer. Meteor. Soc.,* **87,** 343–360, doi:10.1175/BAMS-87-3-343.

Mielke, P. W., 1979: Comment on ''Field experimentation in weather modification.'' *J. Amer. Stat. Assoc.,* **74,** 87–88.

——, L. O. Grant, and C. F. Chappell, 1970: Elevation and spatial variation effects of wintertime orographic cloud seeding. *J. Appl. Meteor.,* **9,** 476–488, doi:10.1175/1520-0450(1970)009<0476:EASVEO>2.0.CO;2.

——, ——, and ——, 1971: An independent replication of the climax wintertime orographic cloud seeding experiment. *J. Appl. Meteor.,* **10,** 1198–1212, doi:10.1175/1520-0450(1971)010<1198:AIROTC>2.0.CO;2.

——, G. W. Brier, L. O. Grant, G. J. Mulvey, and P. N. Rosenzweig, 1981: A statistical reanalysis of the replicated Climax I and II wintertime orographic cloud seeding experiments. *J. Appl. Meteor.,* **20,** 643–659, doi:10.1175/1520-0450(1981)020<0643:ASROTR>2.0.CO;2.

Mooney, M. L., and G. W. Lunn, 1969: The area of maximum effect resulting from the Lake Almanor randomized cloud seeding experiment. *J. Appl. Meteor.,* **8,** 68–74, doi:10.1175/1520-0450(1969)008<0068:TAOMER>2.0.CO;2.

Morel-Seytoux, H. J., and F. Saheli, 1973: Test of runoff increase due to precipitation management for the Colorado River Basin Pilot Project. *J. Appl. Meteor.,* **12,** 322–337, doi:10.1175/1520-0450(1973)012<0322:TORIDT>2.0.CO;2.

Pokharel, B., and B. Geerts, 2014: The impact of glaciogenic seeding on snowfall from shallow orographic clouds over the Medicine Bow Mountains in Wyoming. *J. Wea. Modif.,* **46,** 8–28.

——, ——, and X. Jing, 2014a: The impact of ground-based glaciogenic seeding on orographic clouds and precipitation: A multisensor case study. *J. Appl. Meteor. Climatol,* **53,** 890–909, doi:10.1175/JAMC-D-13-0290.1.

——, ——, ——, K. Friedrich, J. Aikins, D. Breed, R. Rasmussen, and A. Huggins, 2014b: The impact of ground-based glaciogenic seeding on clouds and precipitation over mountains: A multi-sensor case study of shallow precipitating orographic cumuli. *Atmos. Res.,* **147–148,** 162–182, doi:10.1016/j.atmosres.2014.05.014.

Politovich, M. K., and G. Vali, 1983: Observations of liquid water in orographic clouds over Elk Mountain. *J. Atmos. Sci.,* **40,** 1300–1312, doi:10.1175/1520-0469(1983)040<1300:OOLWIO>2.0.CO;2.

Rangno, A. L., 1979: A reanalysis of the Wolf Creek Pass cloud seeding experiment. *J. Appl. Meteor.,* **18,** 579–605, doi:10.1175/1520-0450(1979)018<0579:AROTWC>2.0.CO;2.

——, 1986: How good are our conceptual models of orographic cloud seeding? *Precipitation Enhancement—A Scientific Challenge, Meteor. Monogr.,* No. 43, Amer. Meteor. Soc., 115, doi:10.1175/0065-9401-21.43.115.

——, and P. V. Hobbs, 1987: A reevaluation of the Climax cloud seeding experiments using NOAA published data. *J. Climate Appl. Meteor.,* **26,** 757–762, doi:10.1175/1520-0450(1987)026<0757:AROTCC>2.0.CO;2.

——, and ——, 1993: Further analysis of the Climax cloud-seeding experiments. *J. Appl. Meteor.,* **32,** 1837–1847, doi:10.1175/1520-0450(1993)032<1837:FAOTCC>2.0.CO;2.

Rasmussen, R., and Coauthors, 2001: Weather support to deicing decision making (WSDDM): A winter weather nowcasting system. *Bull. Amer. Meteor. Soc.,* **82,** 579–595, doi:10.1175/1520-0477(2001)082<0579:WSTDDM>2.3.CO;2.

——, and Coauthors, 2011: High-resolution coupled climate runoff simulations of seasonal snowfall over Colorado: A process study of current and warmer climate. *J. Climate,* **24,** 3015–3048, doi:10.1175/2010JCLI3985.1.

——, and Coauthors, 2012: How well are we measuring snow? The NOAA/FAA/NCAR winter precipitation test bed. *Bull. Amer. Meteor. Soc.,* **93,** 811–829, doi:10.1175/BAMS-D-11-00052.1.

——, and Coauthors, 2014: Climate change impacts on the water balance of the Colorado Headwaters: High-resolution regional climate model simulations. *J. Hydrometeor.,* **15,** 1091–1116, doi:10.1175/JHM-D-13-0118.1.

Rauber, R. M., L. O. Grant, D. X. Feng, and J. B. Snider, 1986: The characteristics and distribution of cloud water over the mountains of northern Colorado during wintertime storms. Part I: Temporal variations. *J. Climate Appl. Meteor.,* **25,** 468–488, doi:10.1175/1520-0450(1986)025<0468:TCADOC>2.0.CO;2.

Rhea, J. O., 1978: An orographic model for hydrometeorological use. Ph.D. thesis, Colorado State University Atmospheric Paper 287, 198 pp.

——, 1983: Comments on ''A statistical reanalysis of the replicated Climax I and II wintertime orographic cloud seeding experiment.'' *J. Climate Appl. Meteor.,* **22,** 1475–1481, doi:10.1175/1520-0450(1983)022<1475:COSROT>2.0.CO;2.

Ritzman, J. M., 2013: Estimates of the fraction of precipitation seedable under application of the Wyoming Weather Modification Pilot Project. M.S. thesis, Dept. of Atmospheric Science, University of Wyoming, 114 pp.

Schaefer, V. J., 1946: The production of ice crystals in a cloud of supercooled water droplets. *Science,* **104,** 457–459, doi:10.1126/science.104.2707.457.

Serreze, M. C., M. P. Clark, R. L. Armstrong, D. A. McGinnis, and R. S. Pulwarty, 1999: Characteristics of the western United Stated snowpack from snowpack telemetry (SNOTEL) data. *Water Resour. Res.,* **35,** 2145–2160, doi:10.1029/1999WR900090.

Super, A. B., and J. A. Heimbach, 1983: Evaluation of the Bridger Range winter cloud seeding experiment using control gages. *J. Climate Appl. Meteor.,* **22,** 1989–2011, doi:10.1175/1520-0450(1983)022<1989:EOTBRW>2.0.CO;2.

Thompson, G., P. R. Field, R. M. Rasmussen, and W. D. Hall, 2008: Explicit forecasts of winter precipitation using an improved bulk microphysics scheme. Part II: Implementation of a new snow parameterization. *Mon. Wea. Rev.,* **136,** 5095–5115, doi:10.1175/2008MWR2387.1.

Vonnegut, B., 1947: The nucleation of ice formation by silver iodide. *J. Appl. Phys.,* **18,** 593–595, doi:10.1063/1.1697813.

Weather Modification Incorporated, 2005: Wyoming level II weather modification feasibility study. Final Report to the Wyoming Water Development Commission, Cheyenne, WY, 151 pp. [Available online at http://charybdis.wrds.uwyo.edu/weathermod/Report.pdf.]

Yang, D., B. E. Goodison, J. R. Metcalfe, V. S. Golubev, R. Bates, T. Pangburn, and C. L. Hanson, 1998: Accuracy of NWS 8'' standard nonrecording precipitation gauges: Results and application of WMO intercomparison. *J. Atmos. Oceanic Technol.,* **15,** 54–68, doi:10.1175/1520-0426(1998)015<0054:AONSNP>2.0.CO;2.